Flexural Strength of Light-Weight Steel Fiber Reinforced Concrete Containing Biodegradable LDHs Microparticles: Experimental Study and Multiscale Finite Element Model

Pari Ramazani[1], Taleb Moradi Shaghaghi[1*], Masood Farzam[2], Hassan Afshin[3] and Mohammad A. Behnajady[4]

Abstract

This study investigates the influence of LDHs (Layered Double Hydroxides) microparticles and steel fibers on the mechanical properties of lightweight concrete. Through a combination of experimental analysis and finite element modeling, the effects of LDHs and steel fibers on flexural strength and crack resistance were evaluated. The experimental results demonstrate a significant increase in flexural strength and toughness with the incorporation of LDHs microparticles and steel fibers. The finite element model corroborates these findings, highlighting the synergistic enhancement of mechanical properties due to LDHs and steel fibers. Additionally, the study discusses the frontier applications of LDHs in improving fracture characteristics and highlights the potential of hybrid reinforcement strategies in lightweight concrete. The findings reveal that both the quantity of microparticles and steel fibers significantly impact the concrete's residual strength. In scenarios without steel fibers, an optimal weight fraction of approximately 1 wt.% LDHs demonstrate a 39% increase in bearing capacity. Notably, under comparable conditions, the influence of LDHs microparticles on enhancing concrete mechanical characteristics appears to surpass the effects induced by steel fibers. However, at 2 wt.% LDHs usage, a decrease in load capacity by 3.3% is observed compared to the 1 wt.% LDHs configuration. This research provides valuable insights into optimizing concrete properties through novel material combinations and paves the way for future advancements in structural engineering.

Keywords Lightweight concrete, LDHs microparticles, Multiscale finite element model, Steel fibers, Flexural strength

1 Introduction

Reducing the volumetric weight of concrete in buildings can indeed have a substantial effect on lightening the overall structure. This reduction often leads to advantages such as improved structural efficiency, reduced material usage, and potentially lower construction costs (Huang et al., et al. 2021, 2022). Additionally, it can facilitate easier handling during construction and might even result in more favorable seismic behavior in some cases (Xiao et al., et al. 2023; Zhou et al., et al. 2023a, 2023b). The specific weight of concrete containing porous and lightweight aggregates is significantly lower than ordinary concrete. Concrete, especially lightweight concrete, is considered brittle, as evidenced by its different

Ramazani *et al. Int J Concr Struct Mater*   (2024) 18:37

Page 2 of 16

behavior under tension and compression. For this reason, it is necessary to use an additive that increases the tensile strength of concrete (He et al., et al. 2023, 2024; Pang et al., et al. 2024; Tang et al., et al. 2023). In this area, different additives such as steel slag aggregates, fibers, and microparticles have been extensively investigated (Esmaeili & Andalibi, 2013; Khorshidi et al., et al. 2023a, 2023b; Maleki et al., et al. 2022; Pourreza et al., et al. 2021). Numerous researchers have examined the possibility of improving concrete mechanical and physical properties using nanoparticles and microparticles recently (Esmaeili et al. 2017, Esmaeili et al., et al. 2021).

Various types of fibers serve as supplementary materials for concrete, particularly in lightweight compositions, to enhance its energy absorption capacity upon matrix breakage, addressing this limitation. The inclusion of fibers diminishes crack opening, thereby augmenting the material's fatigue strength (Zhao et al. 2023). Wang et al. (2021) conducted a study comparing the effects of MgO, fly ash, PVA fiber, and shrinkage-reducing admixture on the frost resistance of face slab concrete using pore structural and fractal analysis. Mohamed et al. (2023) explore previous research concerning the integration of steel fibers into lightweight concrete to create sustainable and environmentally friendly concrete solutions. An experimental investigation conducted by Asim et al. (2020) compared natural fiber-reinforced lightweight concrete as thermally efficient building materials. The industrial production of nano/microparticles has led to the emergence of a new area in the use of microparticles in concrete. The effect of nano-silica on the compressive strength of lightweight concrete has been investigated by Du et al. (2015). The results indicate that adding 1% and 2% nano-silica results in an increase of 7.7% and 13.3% in compressive strength, respectively. Certainly, as reviewed Kalpana and Tayu (2020), there have been several studies conducted on the mechanical behavior of lightweight fiber-reinforced concrete. Hamada et al. (2021) investigated the effect of nano-palms on lightweight concrete mechanical properties. This research demonstrates that nano-palm increases the resistance of concrete against cracking. Using a hybrid form of Nano-SiO2, Nano-TiO2, and Nano-Al2O3 nanoparticles, Askari Dolatabad et al. (2020) investigated the rheological and mechanical characteristics of lightweight concrete containing these nanoparticles. By conducting experimental tests, Chu et al. (2023) examined the effect of graphene oxide on the mechanical properties of ultra-strength lightweight concrete. By adding 3% of graphene nanoparticles to the mixture, the bending strength, compressive strength, and elastic modulus are increased by 22.4%, 16.7%, and 13%, respectively. The mechanical properties and microstructure of lightweight concrete containing nano calcium

carbonate were examined by Sldozian et al. (2023). According to Othuman Mydin et al. (2022), lightweight foamed concrete containing Fe3O4 microparticles had higher compressive strength than fiber-reinforced concrete without microparticles. The results showed that the best performance was achieved when Fe3O4 nanoparticles were present at a weight fraction of 0.25%. Liao et al. (2023) investigated the impact of calcined phosphogypsum and slaked lime content variations on the fluidity, setting time, and compressive strength of supersulfated cement. The inclusion of 10% calcined phosphogypsum and 10% slaked lime in supersulfated cement resulted in a compressive strength of up to 35.2 MPa after 180 days. This study elucidates the influence mechanism of calcined phosphogypsum and slaked lime on supersulfated cement hydration, offering theoretical insights crucial for the preparation of supersulfated cement in engineering applications.

Cement composites reinforced with nano/microparticles require considerable production time and are not very cost-effective due to the challenges of spreading the microparticles in the cement bed and the high cost of production. In recent years, the use of finite element and numerical methods has been developed in many different fields (Cui et al. 2023a, 2023b; Li et al. 2024; Lin et al. 2023; Luo et al. 2023; Yang et al. 2023; Zhang et al. 2023a, 2023b, 2023c). The use of numerical modeling techniques is a suitable method for calculating the mechanical properties of many structures and materials such as concrete, given the difficulty and high cost of conducting tests and experiments (Esmaeili et al. 2021; Ren et al. 2022; Yao et al. 2023; Zhang et al. 2023a, 2023b, 2023c). However, the real dimensions of microparticles make finite element modeling difficult in micro and nano dimensions (Du & Jin, 2021; Naderi et al. 2021; Wu et al. 2021). It has also recently been demonstrated that modeling composites as microstructures can be used to predict the mechanical properties of nanocomposites. In this method, the matrix phase and reinforcing particles are simulated separately, and the interactions between them are defined. By defining the properties of both components of the composite, one can determine the mechanical behavior of the material. Khani et al. (2016) investigated the elastic properties of concrete reinforced with spiral and filamentary carbon nanotubes using finite element analysis. The tensile characteristics of fiber-reinforced concrete were investigated by Esmaeili and Andalibi (2019) using a multi-scale finite element method. Wang et al. (2022) established a 3D aggregate database from X-ray CT scans of bulk concrete.

An multi-scale finite element investigation of nanocomposites reinforced with carbon nanotubes was conducted by Vahidi Pashaki et al. (2018). Using two-dimensional simulations, they examined the mechanical

Ramazani *et al. Int J Concr Struct Mater*   (2024) 18:37

Page 3 of 16

behavior of these types of nanocomposites while considering the interaction between microparticles and the matrix. Numerical and Finite element models have been widely used for simulating complex structures under various conditions to enhance structure performance in real-world applications, ranging from biomechanical simulation, crucial for understanding pathological conditions (Abbasi-Ghiri et al. 2022; Razi et al. 2023; Saghafian et al. 2023; Wu et al. 2023) and the development of innovative medical devices (Ebrahimkhani et al. 2020), to structural models, which are pivotal in enhancing the structural integrity and performance of modern construction materials, as discussed here. Esmaeili et al. (2021) studied the influence of steel fiber geometric characteristics on fiber-reinforced concrete behavior using the multi-scale finite element method. Meso-scale representative volume elements of straight and coiled CNT-reinforced epoxy composites were analyzed by Haydar (2021) via commercial finite element analysis software. According to their model, there is a limit to the number of microparticles. Adhikary et al. (2021) investigated the effects of carbon nanotubes and graphene nanosheets on the mechanical behavior of lightweight concrete. The effect of carbon nanotubes on the mechanical and thermal properties of lightweight structural concrete containing silica particles was investigated experimentally by Shahpari et al. (2022). The thermodynamic database of ordinary Portland cement-based materials serves as the foundation for simulating the hydration products of the low-heat Portland cement paste explored by Zhou et al. (2023a, 2023b), employing the thermodynamic software GEM-Selektor for this analysis. The initial and final stages of low-heat Portland cement pastes at a micro level are visualized by MATLAB. Peng et al. (2022) investigate the impact of the magnesium–phosphorus molar ratio and water-to-binder ratio on the hydration products through thermodynamic simulation.
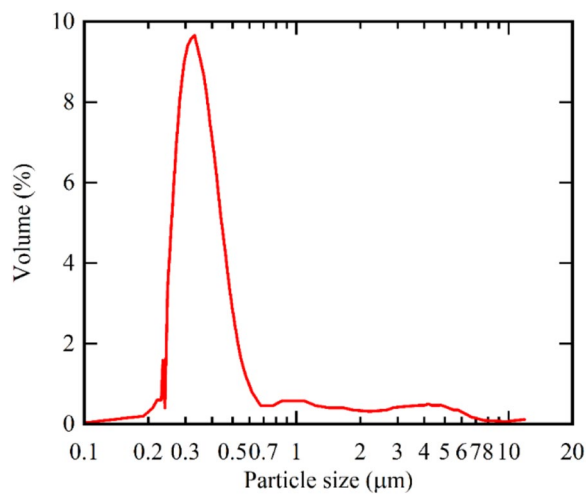
Layered Double Hydroxides (LDHs) are a class of synthetic inorganic compounds characterized by a layered structure. They belong to the family of anionic clays and are composed of positively charged metal hydroxide layers with intercalated anions and water molecules between the layers. The basic structure of LDHs consists of positively charged layers, typically containing divalent and trivalent metal cations (such as magnesium, aluminum, zinc, or iron), which are balanced by exchangeable anions like carbonate, chloride, or nitrate ions, among others. These layers are stacked in a repeating pattern, forming a layered structure resembling a sandwich or a book with alternating positively charged layers and interlayer spaces (Laipan et al. 2020). One distinctive feature of LDHs is their ability to undergo ion exchange, meaning that the anions in the interlayer space can be replaced or exchanged with different anions without altering the overall structure. This property allows LDHs to be functionalized or modified with various organic or inorganic species, making them versatile materials in different applications (Laipan et al. 2020). LDHs have garnered attention across various fields, including materials science, catalysis, medicine, and environmental science, due to their unique properties such as high surface area, tunable chemistry, and potential for controlled release of substances. In construction materials like concrete, LDHs can be used as additives to enhance mechanical properties, durability, and sustainability (Tang et al. 2020).

It's evident from the review of existing studies that there has been limited exploration into the mechanical behavior of lightweight concrete reinforced with microparticles. Furthermore, the impacts of utilizing various types of microparticles in lightweight concrete remain relatively unexplored. Most studies have relied on time-consuming and costly experimental tests, without considering the application of finite element methods in this domain. This study pioneers the use of the multi-scale finite element method to examine the influence of LDHs microparticles on the bending characteristics of lightweight fiber-reinforced concrete (LWFRC). This novel approach aims to fill the gap in understanding the effects of microparticles on the mechanical behavior of lightweight concrete, offering a more efficient and analytical means of investigation compared to traditional experimental methods. Using this method, concrete mortar is modeled as a homogeneous material within which fibers and microparticles are randomly distributed according to their weight fractions. Finite element models were constructed employing the ABAQUS software, integrating the Cohesive Zone Model (CZM) to replicate fiber adhesion within the concrete matrix and the Tie model to emulate microparticle adhesion with the concrete matrix. To validate the accuracy of the numerical model, a three-point bending experiment was conducted on notched Lightweight Fiber-Reinforced Concrete (LWFRC) beams reinforced with LDHs microparticles. After calibrating and validating the finite element model against experimental data, the study will delve into examining various parameters. These include exploring the impact of parameters such as the weight fraction of fibers and microparticles, alongside the adhesion of fibers to the concrete matrix. This comprehensive investigation aims to elucidate the influence of these parameters on the mechanical behavior of the composite material, offering insights into the optimal configurations for enhancing its structural performance.

Ramazani *et al. Int J Concr Struct Mater*   (2024) 18:37

Page 4 of 16
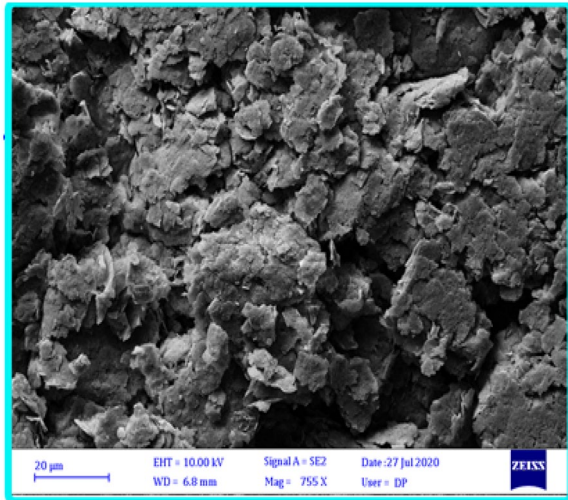
Fig. 1 Scanning electron microscope image of LDHs microparticles

Fig. 3 Structure of the synthetic-based lightweight LECA grains

Fig. 4 Geometry of the steel microfibers

Fig. 2 Size distribution of LDHs microparticles

Table 1 Physical and mechanical characteristics of steel fibers

Poison ratio	Young modulus	Tensile strength	Aspect ratio	Length	Diameter
0.29	208 GPa	1228 MPa	120	60 mm	0.5 mm

2 Experimental Tests

2.1 LDHs Microparticles

Microparticles of ZnAl LDHs with grain sizes between 300 and 600 nm were utilized, which were supplied by DRN Technologies Sdn Bhd and had a purity greater than 99%. Fig. 1 illustrates an image of LDHs microparticles captured by a scanning electron microscope. As shown in the figure, the microparticles possess an almost hexagonal layered structure. According to Fig. 2, LDHs particles range in size from 300 to 600 nm, with the majority measuring 330 nm.

2.2 Materials and Mixture Proportions

The samples were made using Type II Portland cement. This cement has a specific weight of 3150 kg/m^3 and a specific surface area of 0.306 m^2/gr. LECA has been used for coarse lightweight aggregate within the standard range of ASTM C330-00 with a specific density of 350 kg/m^3. A view of the microstructure of the synthetic light grains of LECA is shown in Fig. 3. The fine aggregate utilized in concrete was river-type sand. A polycarboxylate-based superplasticizer of Carboxal HF5000 density of 1.1 ± 0.2 gr/cm^3 was added at varying rates to achieve the required workability. The straight steel fibers (SF) shown in Fig. 4 are used in this study. Fiber density is 7850 kg/m^3 and the physical characteristics of these fibers are presented in Table 1. Table 2 gives the weight values of the materials used based on ASTM-C330-00, (2017) and ACI 211-2 (Prestera et al., et al. 1998).

Ramazani *et al. Int J Concr Struct Mater*   (2024) 18:37

Page 5 of 16

Table 2 Mix the recipe of the LWFRC with LDHs microparticle

| Mix No.	Density (kg/m³)	SP	w/c	LECA (kg/m³)	Sand (kg/m³)	Steel fibers (%)	LDHs (wt.%)	Cement (kg/m³)
LWC-LDHs0-SF0	1748	4	0.33	432	735	0	0	400
LWC-LDHs0.5-SF5	1782	4	0.33	429	731	0.05	0.5	398
LWC-LDHs2-SF10	1831	4	0.33	427	727	0.1	2	396

The process entails pre-mixing LDHs in water before their incorporation into concrete. Nanomaterial dispersion in water is facilitated by employing the ultrasonic method. Initially, the necessary quantity of LDH microparticles is weighed and placed into an oven. Subsequently, a specific amount of water is added to the particles, and the combination is inserted into an ultrasonic device. Adequate mixing is achieved after approximately 30 min at a frequency of 10 kN.

2.3 Three-Point Bending Test

To evaluate the bending strength of LWFRC rectangular beam samples reinforced with LDHs microparticles, three-point loading tests were conducted. In Fig. 5, the experimental setups and geometric dimensions of the samples are illustrated. By ASTM C1018 (ASTM, 1998), a displacement control load is applied at a loading rate of 0.2 mm/min. To determine the bending strength of various samples, the force–displacement curve and load-crack mouth opening displacement (CMOD) were measured.

The finite element model in this study consists of three distinct phases, namely cement mortar, microparticles, and fibers. Thus, by performing compressive and tensile experimental tests, the mechanical
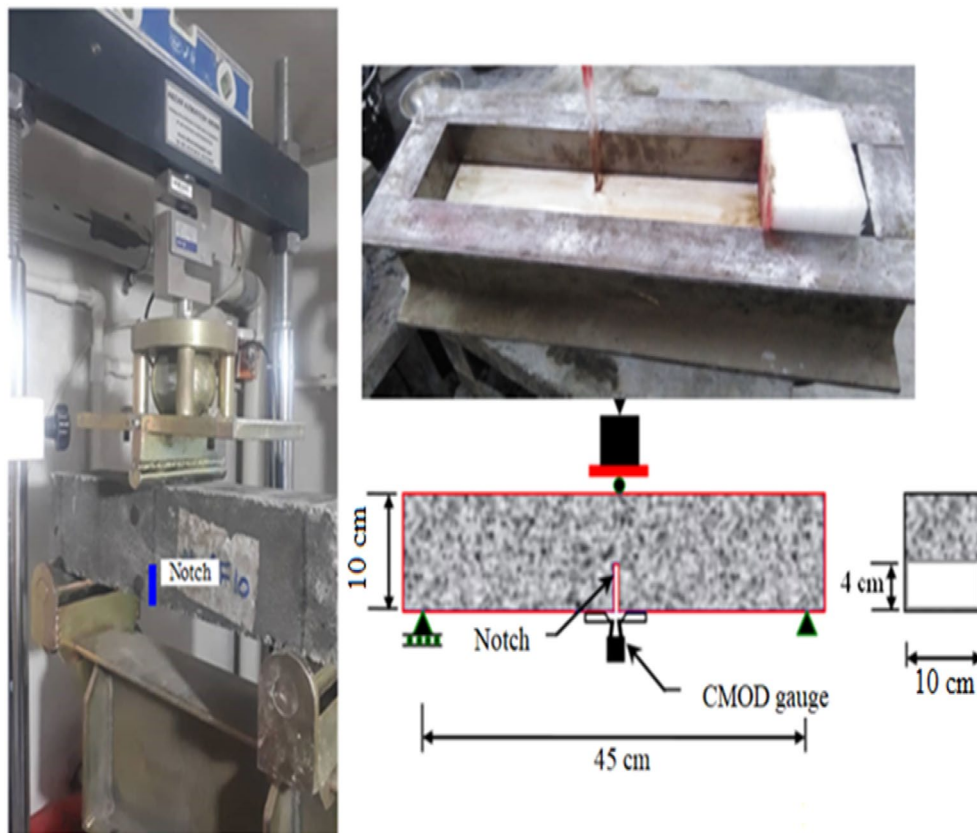

Fig. 5 The geometrical dimensions and the three-point bending laboratory setup of the LWFRC beam reinforced with LDHs microparticles

Ramazani *et al. Int J Concr Struct Mater* (2024) 18:37

Page 6 of 16

characteristics of cement mortar can be determined separately and input into software (Fig. 6).

3 Multiscale Finite Element Model

In this section, multiscale finite element simulations of LWFRC beams reinforced with LDHs microparticles are discussed using ABAQUS software. Simulated beam dimensions and geometric characteristics are similar to those of the laboratory conditions of the three-point bending of a rectangular notched beam. This model includes a concrete beam, fibers, and microparticles, and
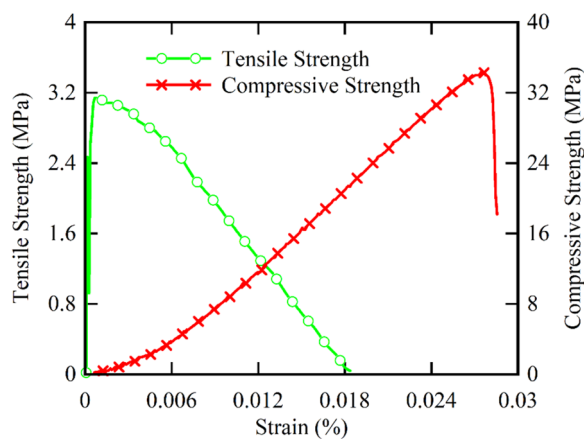
Fig. 6 Compressive and tensile stress–strain curve of lightweight concrete without fibers and microparticles

three solid bodies acting as hydraulic jacks and supports, as illustrated in Fig. 7.

The current study uses a multi-scale finite element model to examine the mechanical behavior of LWFRC reinforced with LDH microparticles. Fibers and microparticles with random distribution are individually placed beside each other in this method. To simulate realistic conditions of the presence of fibers and microparticles in lightweight concrete, the orientation, as well as the number of fibers and microparticles, have been created irregularly and randomly. To define the interaction between fibers and cement mortar, adhesive elements based on CZM were used. Because microparticles adhere to cement mortar with a strength greater than aggregate fracture strength, this area has been given the Tie constraint. MATLAB and the Script environment of ABAQUS software were used to create a three-dimensional geometric model of the distribution of fibers and microparticles inside the concrete context. Fibers are modeled as cylindrical cylinders and aggregates are represented as hexagonal particles within the base material.

A geometric model of the random distribution of fibers and microparticles created using the mentioned algorithm is shown in Figs. 8 and 9, for different weight fractions in percentage (wt.%) of steel fibers and microparticles. The three-dimensional geometry makes it possible to place fibers and microparticles in different orientations, lengths, and spatial positions. As can be seen in the figure, using the proposed algorithm, fibers
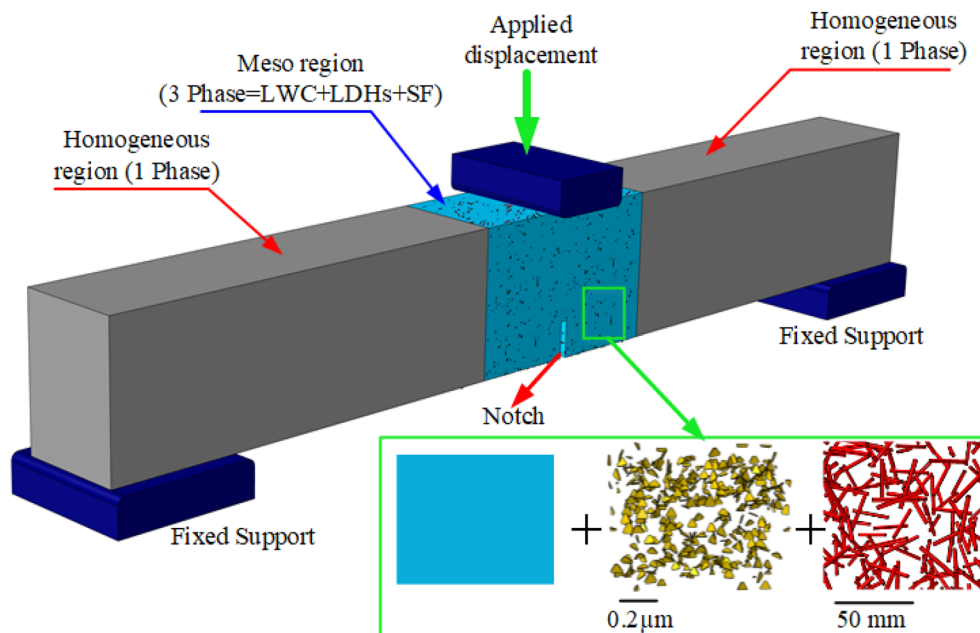

Fig. 7 Details of multiscale finite element simulation of three-point bending of the fiber-reinforced lightweight concrete beam with LDHs microparticles

Ramazani *et al. Int J Concr Struct Mater*   (2024) 18:37

Page 7 of 16
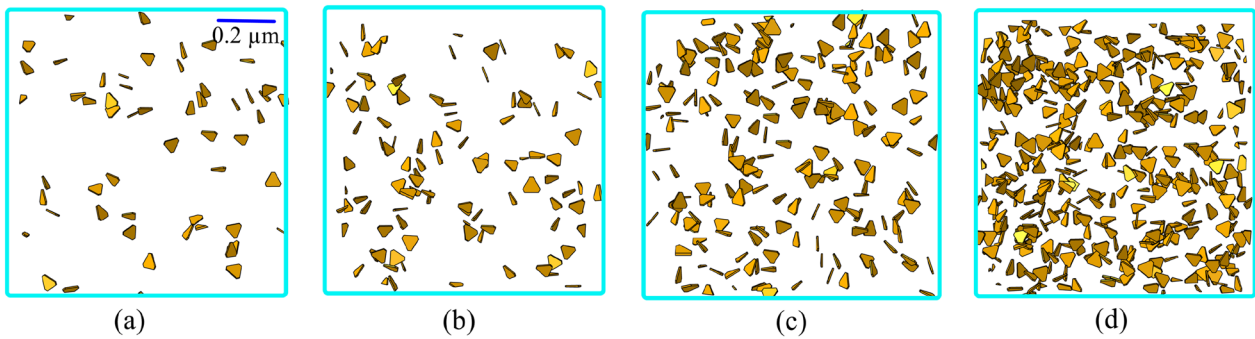
Fig. 8 LDHs microparticles dispersion with different weight fractions in percentage (wt%) of cement, **a** 0.2 wt.%, **b** 0.5 wt.%, **c** 1 wt.% and **d** 2 wt.%
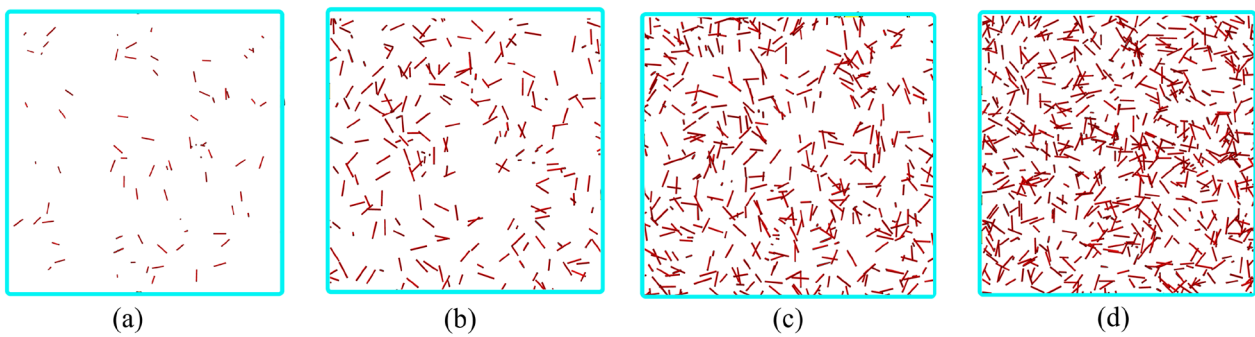
Fig. 9 Steel fiber distribution with different weight fractions in percentage (wt.%) of cement, **a** 0.2 wt.%, **b** 0.5 wt.%, **c** 1 wt.%, and **d** 2 wt.%
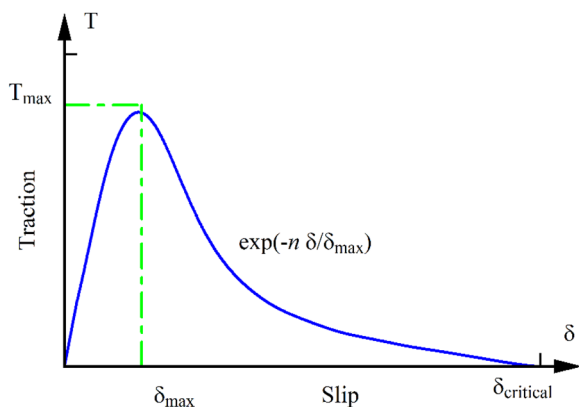
Fig. 10 Traction–separation in the adhesion area

are placed at random within the concrete matrix, and from this point of view, this type of distribution can accurately predict fiber distribution in the experimental condition.

The adhesive zone model theory has been used to model the phenomenon of separation between fibers and concrete in the contact area. Fig. 10 illustrates the traction–separation curve for this model. This model assumes that all of the mechanisms involved in the fracture process are expressed by four parameters, as shown in Fig. 10. These parameters are (1) the strength of the adhesive area (T_{max}), (2) the critical separation distance (δ_{max}), and (3) the parameter of n indicating how fracture area changes exponentially. A further parameter of the adhesive zone model is Gc, which is the separation energy. Following the calibration of the finite element model based on experimental results and determining the parameters of the adhesive zone model and the constants of the adhesion behavior model between fibers and lightweight concrete, a finite element study of the effects of different parameters on the behavior of lightweight concrete reinforced with fibers is conducted.

The Concrete Damaged Plasticity constitutive model was used for lightweight concrete mortar, which accounts for both the tensile and compressive properties of concrete separately (see Fig. 6). Furthermore, fibers are assumed to be elastic–plastic, while microparticles of LDHs are assumed to be fully elastic. Considering geometrical nonlinearities, the dynamic/explicit solution method has been used to perform finite element analysis. A surface-to-surface contact is defined as the contact between a beam and rigid components. Two lower supports are fully restrained, and the displacement boundary condition is applied to the rigid body above the beam. The model meshed using ten-node C3DPE10M nonlinear pyramidal elements as a result of

Ramazani *et al. Int J Concr Struct Mater* (2024) 18:37

Page 8 of 16

the geometric complexity of the structure. To determine the appropriate size of the elements, the grid independence is checked, and 1,459,803 elements are used in the final mesh. Through the application of static loading on the samples, this study aims to investigate the influence of several parameters on the bending strength.

4 Finite Element Model Updating

Model updating is an optimization problem in which the mechanical properties of the structure are used as optimization variables. Using this model, it is possible to develop an accurate finite element model that takes into account the uncertainties in the laboratory model and the existing errors. The CZM parameters, including and *n*, are determined in the current study in a manner that minimizes the difference between the maximum force and fracture energy obtained from the finite element analysis and the experimental results. ABAQUS and MATLAB are used to solve this optimization problem. The steps involved in updating the finite element model are illustrated in Fig. 11. To optimize the objective function, the Nelder-Mead algorithm and fmincon function of MATLAB software are used. The refined finite element model is derived by identifying optimal system parameter values that minimize the disparities between the results obtained from both the finite element simulations and experimental models.

5 Validation

The results of the finite element model and experimental testing are presented in this section. According to Fig. 3, the term LWC-LDHs**-SF** is used. The first letter represents lightweight fiber concrete, the second letter represents the weight fraction in percentage (wt%) of cement of LDHs microparticles, and the third letter represents the weight fraction of steel fibers.

5.1 Experimental Results

A three-point bending test was conducted on three LWFRC samples with the specifications listed in Table 2. The load–displacement diagrams obtained from the bending strength test for these three samples, namely LWC-LDHs0-SF0, LWC-LDHs0.5-SF5, and LWC-LDHs2-SF10 are presented in Fig. 12. Energy absorption or toughness is represented by the area under these graphs. In the base sample, the area under the load–displacement curve is approximately 6.5 N.m, while in the sample containing 0.5 wt.% LDHs and 5 wt.% steel fiber, the area under the curve is approximately 39.5 N.m. In which wt.% represents the weight fraction in percentage (wt%) of cement. LDHs fibers and microparticles
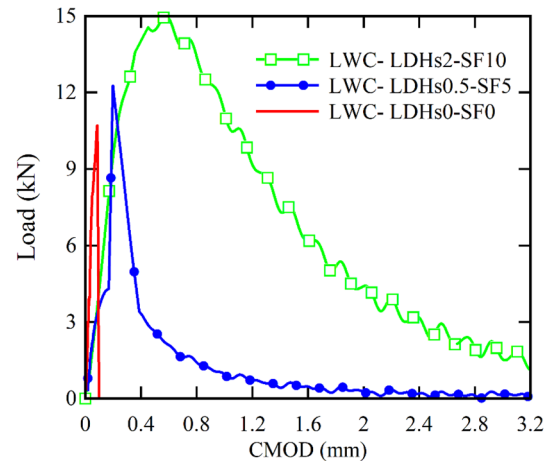
Fig. 12 Load–displacement diagrams obtained from the three-point bending test for different light concrete samples
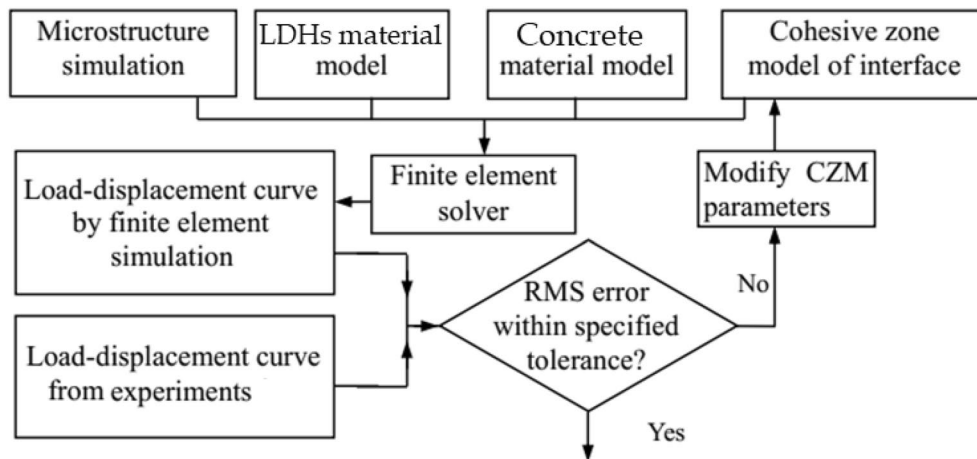
Fig. 11 The process of the multiscale finite element model updating

Ramazani *et al. Int J Concr Struct Mater* (2024) 18:37

Page 9 of 16

contribute significantly to the toughness of lightweight concrete in this study. It can be concluded that LDHs microparticles significantly increase the bending strength and toughness of the material. According to the figure, we can also see that when the percentage of LDHs microparticles in light concrete increases, the bending strength and maximum load that can be tolerated by the beam samples will increase. A simple beam sample and a beam reinforced with microparticles of LDHs with 0.5 wt.% and 2 wt.% have bearing capacities of 10.6 kN, 12.24 kN, and 14.69 kN, respectively. Additionally,

because fibers increase the displacement of the middle of the beam opening, LWFRC reinforced with fibers will be more ductile before failure.

5.2 Validation of Multiscale Finite Element Model
Using the contact constraint and the definition of adhesive elements, the interaction between fibers and concrete was modeled in the presented multi-scale finite element model. The parameters of the CZM adhesive zone model were determined using the model updating method in a manner that is consistent with the force–displacement curve obtained from the finite element model. Table 3 presents the adhesive zone model parameters based on the three-point bending test results. Based on the values in Table 3, Fig. 13 illustrates the force-slip curve of the final finite element model and the results of the experimental tests conducted on control samples as well as on LWC-LDHs0.5-SF0.5 and LWC-LDHs2-SF1. The results of the laboratory sample and the finite

Table 3 CZM parameters to define the interaction of steel fibers with lightweight concrete

	T_{max}	δ_{max}	G_c	n
Steel fiber	3.42 MPa	1.8×10^{-3} mm	0.36 MPa mm	3.03
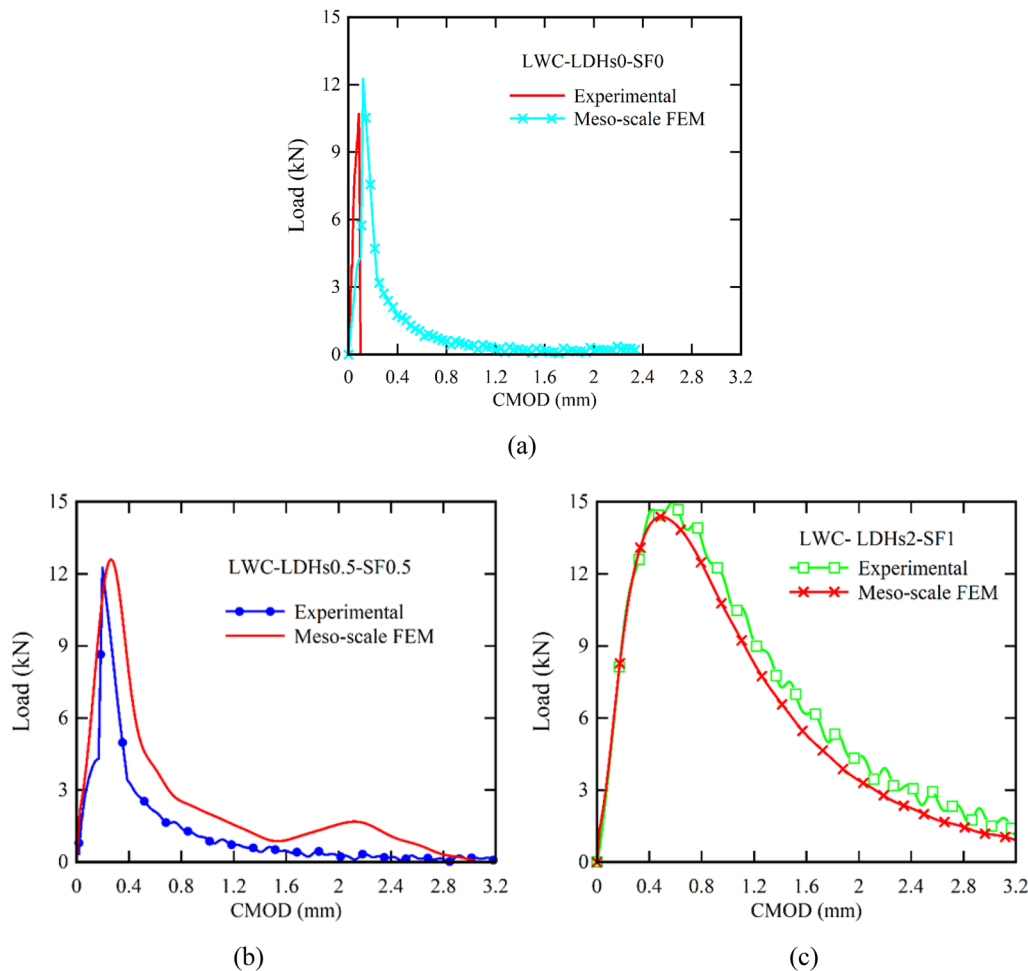
Fig. 13 Force–displacement curve of experimental tests and multiscale finite element model **a** lightweight concrete without fibers and **b**, **c** lightweight concrete reinforced with fibers

element model have a favorable overlap, and the method of updating the model has a suitable level of accuracy in predicting lightweight fiber-reinforced concrete mechanical behavior. This model was updated based on the results of the LWC-LDHs0.5-SF0.5 sample, and the LWC-LDHs2-SF1 sample was used to verify its accuracy. As a result of the finite element analysis, we can determine that the maximum force for LWC-LDHs0.5-SF0.5 and LWC-LDHs2-SF1 samples is 12.48 kN and 14.44 kN, respectively, with an error of 4.3% and 2.4%, respectively. Differences between numerical and experimental results may arise from factors like model assumptions, material properties, boundary conditions, and complexities in simulating real-world behavior. Also, Complex fracture and failure mechanisms in concrete and composite materials might be challenging to simulate accurately, leading to differences between numerical and experimental outcomes.

5.3 Crack Growth in Notched Samples

A multi-scale finite element method is presented in Fig. 14 for predicting the failure position of fiber-reinforced concrete beams under three-point bending loading. Based on the finite element analysis and experimental results, the failure mode of LWC-LDHs0.5-SF0.5 and LWC-LDHs2-SF1 samples under three-point bending loading is depicted. In comparing the presented finite element model with the experimental failure mode of the corresponding sample, the present model accurately predicts the failure mode and crack growth position. Accordingly, the present multiscale finite element model accurately simulates the bending behavior of LWFRC reinforced with microparticles when subjected to three-point bending loading. Generally, the introduction of

LDHs expedites the hydration process, yielding enhanced mechanical properties and a more refined pore structure in cement-based materials. These effects stem from the pore-filling and nucleation mechanisms attributed to LDHs. Studies have indicated that microfillers smaller than 0.3 μm contribute to a pore-filling effect, thereby refining the microstructure of cement-based materials (Quercia et al., et al. 2012). The control of LDHs particle size below 500 μm through methodological improvements, enabling effective pore structure refinement. Additionally, LDHs typically possess nano-scale thickness, serving as nucleation sites that expedite the uniform formation of hydration products.

Fig. 15 shows the crack growth in samples of LWC-LDHs0.2-SF1, LWC-LDHs0.2-SF1.5, and LWC-LDHs0.2-SF2. Results show that the weight fraction of fibers affects the path of crack growth in LWFRC beams, and the maximum strength and crack length decrease significantly as fiber volume increases. Crack propagation was instantaneous and fast in the samples without fibers, failing immediately after the first crack appeared. The samples with fibers, on the other hand, can bridge cracks due to the long length of the steel fibers after the first crack and after the crack grows. As a result of its high tensile strength, the concrete can prevent cracks from growing and spreading, thereby increasing its bending strength and formability.
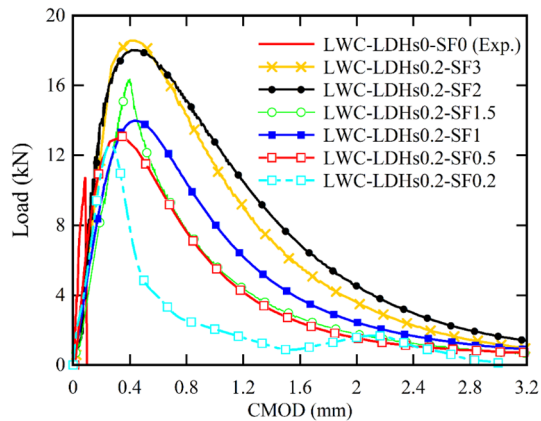
5.4 P-CMOD Curves

P-CMOD curves for notched LWFRC beams for different fiber weight fractions are shown in Fig. 16. Based on the results, it is apparent that the bearing capacity of the beam significantly increases with an increase in the weight fraction of fibers. Despite having higher fracture
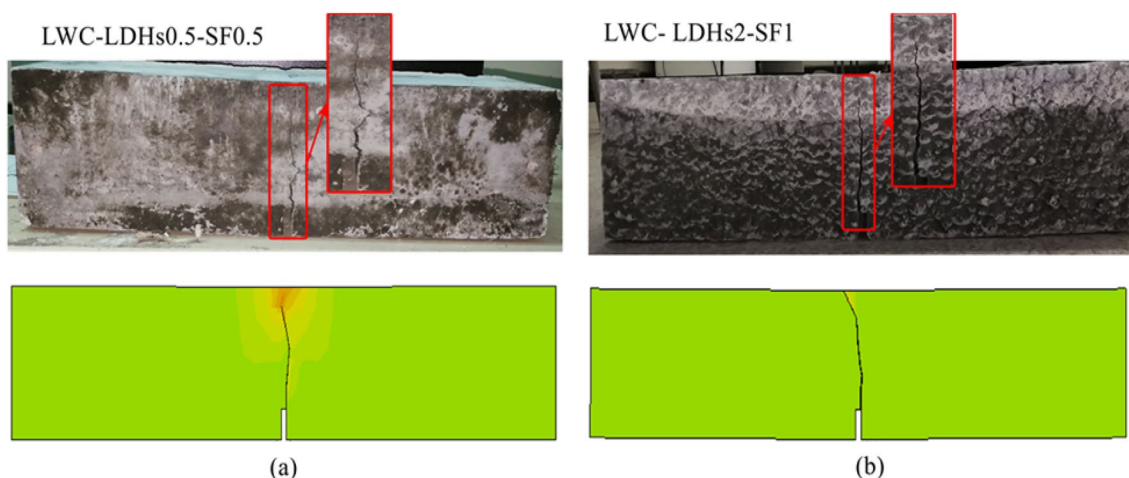
Fig. 14 Comparison of experimental results and multi-scale finite element failure of LWFRC reinforced with LDHs microparticles **a** LWC-LDHs0.5-SF0.5 and **b** LWC-LDHs2-SF1
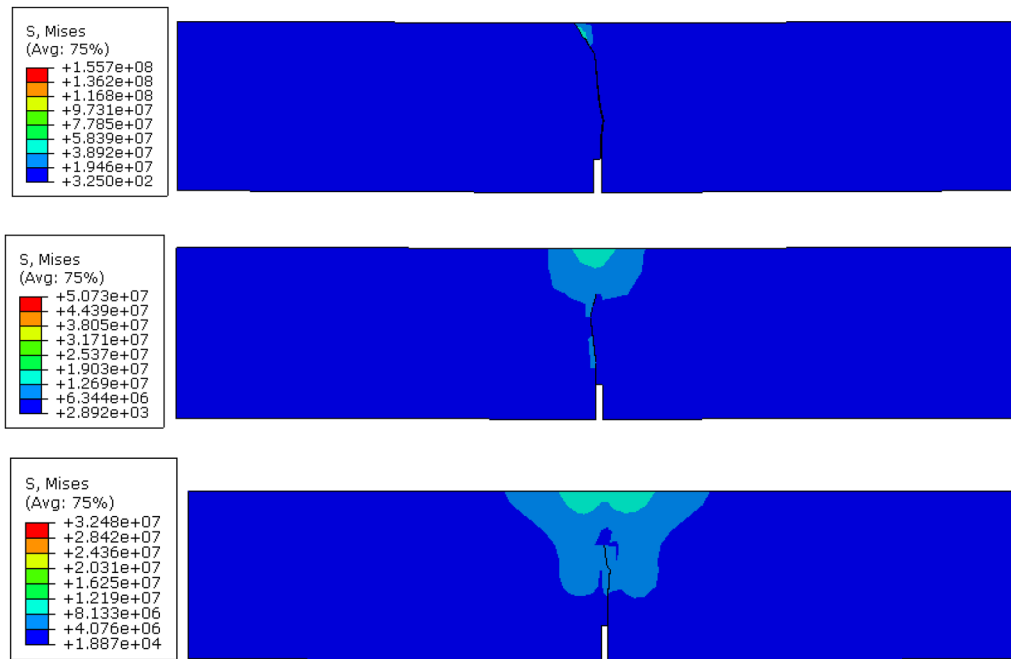
**Fig. 15** Crack growth in LWC-LDHs0.2-SF1, LWC-LDHs0.2-SF1.5 and LWC-LDHs0.2-SF2 for 15 kN force

Fig. 16 Load–CMOD curve for notched LWFRC beams reinforced with LDHs microparticles for different fiber content

energy due to fiber bridging, lightweight concrete with a larger weight fraction of fibers exhibits a much better behavior after the peak point, as can be seen in Fig. 16. During the crack opening, fiber bridging energy is required to pull-out the fibers from the concrete. In the case of high amounts of fibers, the softening slope of the curve has two failures, caused by the effect of fiber bridging on the samples' bending strength. Specimens containing fibers have residual strength, which means that after reaching the maximum force, the beam will still be able to resist the force. The residual strength of fiber concrete

is due to the fibers' resistance to rapid crack growth. It is important to note that as the crack length increases, the adhesion of concrete decreases, and fibers begin to play an increasingly important role in bearing the applied load. In addition to increasing the applied force, some of that force will be used to stretch the fibers away from the concrete, which will result in a reduction in the growth rate of cracks. Upon complete damage to the fiber–concrete interface, the fibers separate from the concrete, and a crack begins to grow. Additionally, with increasing fiber weight fraction, the displacement of the middle of the opening corresponding to the maximum load increases, resulting in greater ductility before failure. A comparison of the load-CMOD curves of the samples indicates that the descending branch of the control sample curve shows a significant softening strain with an increase in fiber content. The behavior of this behavior is modified by the inclusion of fibers in the samples, which results in a softer fracture and a larger load-CMOD curve area. As a result, it enhances the energy absorption capacity of LWFRC when under maximum load. Therefore, it can be stated that with the increase in the weight fraction of fiber content, the plasticity and fracture behavior of concrete appear as soft ductile materials.

The P-CMOD curve for notched LWFRC beams at different amounts of LDHs microparticles is shown in Fig. 17. For certain amounts of steel fibers, it can be seen that adding LDHs microparticles increases their bearing capacity. By adding 1 wt.% LDHs, the bearing capacity of
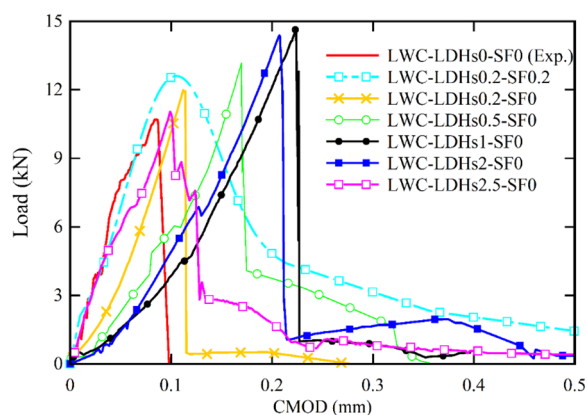
Fig. 17 Load–CMOD curve for grooved fiber reinforced concrete beams for different amounts of weight fraction of LDHs microparticles

these beams is increased by 37% in the absence of steel fibers. Due to the microstructure of lightweight concrete and the presence of nanometer-sized holes in it, this type of nanoparticle fills very small pores and even voids that are nanometer-sized in concrete, and by creating a denser structure, lightweight concrete can achieve better mechanical performance. The high specific surface area and surface energy of LDH microparticles cause the microparticles to act as atomic nuclei and cause strong adhesion between concrete components. Due to the resistance of microparticles against the growth of microcracks, lightweight concrete exhibits enhanced mechanical properties as a result of this effect. As shown in Fig. 17, the excessive increase of LHD microparticles weakens the mechanical properties of lightweight concrete. When 2 wt.% LDHs are used, load capacity is decreased by 3.3% in comparison to 1 wt.% LHDs. Therefore, an increased dosage of LDHs had an adverse impact on their uniform distribution within the cement paste,

consequently diminishing the strength of the hardened cement.

A load-CMOD diagram can be used to measure different parameters, an example of which is shown in Fig. 18 based on EN14651 standards. Using the load-CMOD curve, the residual strength parameter is determined for four CMOD values of 0.5, 1.5, 2.5, and 3.5 mm. Detailed information regarding the residual flexural strength of the different samples is presented in Table 4. In the presence of steel fibers and for a minimum weight fraction of LDHs microparticles of 0.2 wt.%, the failure mode changed from brittle to ductile. If the amount of LDHs is less than 0.2 wt.%, the residual strength will be much lower, causing brittle failure in the material, and the use of fibers in this case may not be of great benefit.

Two factors determine the residual strength of a light fiber concrete beam: the first is the strength of the fibers themselves, and the second is the strength of the adhesive between the fibers and concrete. Using finite element models, it has been observed that steel fibers do not break during crack growth, indicating that the tensile strength of fibers is greater than the external force of fiber elongation. Accordingly, it is concluded that residual strength in light fiber concrete is primarily determined by its ability to extend fibers from concrete, and if the adhesive force between fibers and concrete can be increased, the residual strength of these concretes and fracture toughness will be significantly enhanced. To create the possibility of fiber bridging in concrete, the amount of LDHs microparticles should be greater than 0.2 wt.%. Compared to the control sample, LWC-LDHs1-SF1 and LWC-LDHs1-SF2 exhibit a 61% and 122% increase in maximum strength, respectively, showing that LDHs microparticles significantly increase the bearing capacity of light fiber concrete beams reinforced with microparticles. Increasing the amount of LDHs microparticles from 0.2 wt.%
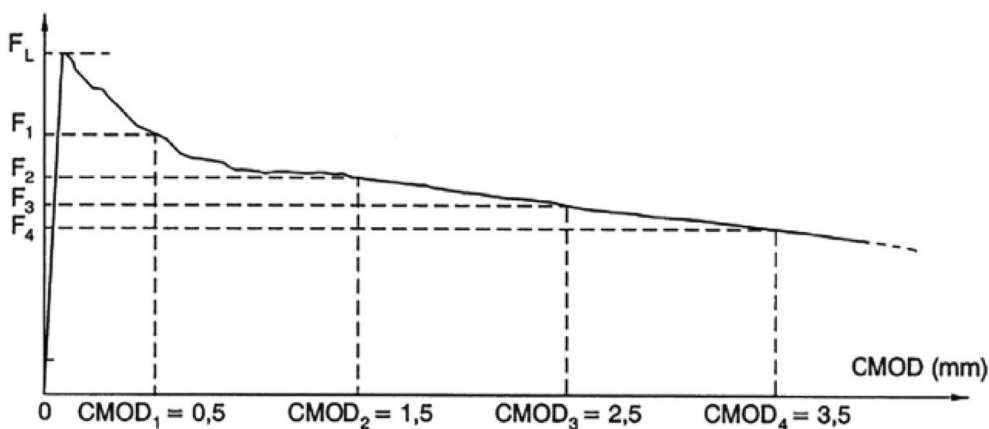
Fig. 18 Typical load–CMOD curve (Di Maida et al. 2018)

Table 4 parameters of the load-CMOD curve and residual strength according to EN 14651

Sample ID	The wt.% of fiber content (%)	The wt.% of LDHs content (%)	F_{max} (kN)	Load increase (%)	F_i			
					F_1 (0.5 mm)	F_2 (1.5 mm)	F_3 (2.5 mm)	F_4 (3.5 mm)
LWC-LDHs0-SF0	–	–	10.56	–	–	–	–	–
LWC-LDHs0.1-SF0	0.0	0.1	11.24	6.44	–	–	–	–
LWC-LDHs0.2-SF0	0.0	0.2	11.98	13.45	–	–	–	–
LWC-LDHs0.5-SF0	0.0	0.5	13.17	24.72	–	–	–	–
LWC-LDHs1-SF0	0.0	1	14.76	39.77	–	–	–	–
LWC-LDHs2-SF0	0.0	2	14.38	36.17	0.38	–	–	–
LWC-LDHs2.5-SF0	0.0	2.5	11.04	4.55	0.41	–	–	–
LWC-LDHs0.2-SF0.5	0.5	0.2	13.02	23.30	11.65	2.75	1.00	0.62
LWC-LDHs0.5-SF0.5	0.5	0.5	14.57	37.97	12.78	4.56	3.45	2.39
LWC-LDHs1-SF0.5	0.5	1	15.34	45.27	14.40	6.97	4.01	1.54
LWC-LDHs2-SF0.5	0.5	2	13.74	30.11	10.2	3.03	1.03	-
LWC-LDHs0.2-SF1	1	0.2	13.98	32.39	13.79	4.26	1.52	0.76
LWC-LDHs0.5-SF1	1	0.5	15.23	44.22	14.98	7.45	5.67	2.04
LWC-LDHs1-SF1	1	1	17.02	61.17	16.23	10.37	8.03	3.45
LWC-LDHs2-SF1	1	2	14.34	35.80	11.23	8.56	4.65	1.14
LWC-LDHs0.2-SF2	2	0.2	18.09	71.31	17.87	7.64	2.67	1.08
LWC-LDHs0.5-SF2	2	0.5	20.31	92.33	19.51	11.34	6.35	2.85
LWC-LDHs1-SF2	2	1	23.45	122.06	21.09	15.65	10.23	5.27
LWC-LDHs2-SF2	2	2	21.34	102.08	18.84	10.03	5.85	2.93

to 1 wt.% increases the carrying capacity by approximately 30% for a fiber weight fraction of 2 wt.%. Since the mechanical properties are reduced with 2 wt.% of LDHs, it can be argued that determining the optimal amount of microparticles will reduce the use of microparticles and as a result reduce economic costs. The authors posited that LDHs could contribute to filling and nucleation effects within the cement paste, potentially enhancing the compressive and flexural strength of the mortar. However, in instances where the mortar included LDHs with a minimum particle size (0.3 μm), the strength declined beyond an LDH dosage of 2.0%. This decrease was linked to LDH aggregation within the mortar, undermining the potential strength-enhancing effects of LDHs.

Analysis from Table 4 is insightful in comparing the effects of LDHs microparticles and steel fibers on the maximum force in the concrete. It seems that increasing the amount of LDHs microparticles from 0.5 wt.% to 1 wt.% resulted in a significant rise in the maximum force, showing a 12% improvement. Meanwhile, a similar increase in the amount of steel fibers (from 0.5 wt.% to 1 wt.%) resulted in a 5.3% increase in the maximum force. From these findings, it's evident that under the same conditions, the impact of LDHs microparticles on enhancing the mechanical characteristics of concrete appears to surpass the effect induced by steel fibers. This comparative analysis highlights the potential significance of LDHs microparticles in improving the overall strength of the concrete structure.

6 Conclusion

Fiber-reinforced lightweight concrete is distinguished by its behavior in the cracked tensile zone, called tensile softening behavior. There have been numerous studies conducted on this behavior and several softening models have been presented. A multiscale finite element model has been developed to investigate the bending behavior and crack propagation of LWFRC notched beams reinforced with LDHs microparticles. The finite element model is composed of three phases: cement mortar, LDHs microparticles, and steel fibers, which are distributed randomly and have a specific weight fraction in the beam. A CZM concept was used to develop the interface between fibers and cement mortar. The parameters of the CZM model were determined by updating the model and minimizing the difference between the finite element model results and the experimental results.

A multiscale finite element model developed in this study predicts the behavior of crack propagation and failure in LWFRC beams reinforced with LDHs microparticles with high reliability and appropriate accuracy. A fiber-reinforced concrete sample with a greater weight fraction of fibers displayed a much better failure behavior than other samples, but the use of this sample is costly.

Ramazani *et al. Int J Concr Struct Mater* (2024) 18:37

Page 14 of 16

As a result, the use of LDH microparticles in conjunction with fibers was recommended in this study. Based upon the parametric study of the effects of nanoparticle weight fraction and steel fibers on load-CMOD curves of different samples, it has been found that the maximum load is achieved by increasing the amount of LDH microparticles to 1 wt.% and for 1 wt.% and 2 wt.% of steel fibers, the beam's strength increased by 61% and 122%, respectively. Accordingly, LDH microparticles have a significant impact on the bending characteristics of fiber-reinforced lightweight concrete beams compared to the control sample. When the weight fraction of LDH microparticles exceeds 1 wt.%, the bearing capacity of the beams decreases. For lightweight concrete to achieve the highest flexural properties, 1 wt.% of LDHs microparticles should be used.

Declarations

Ethics approval and consent to participate
Not applicable.

Informed consent
Informed consent was obtained from all individual participants included in this study.

Consent for publication
All the authors agree that the article will be published after acceptance.

Competing interests
The authors declare that they have no competing interests.

References
Abbasi-Ghiri, A., Ebrahimkhani, M., & Arjmand, N. (2022). Novel force–displacement control passive finite element models of the spine to simulate intact and pathological conditions; comparisons with traditional passive and detailed musculoskeletal models. *Journal of Biomechanics, 141*, 111173.

Adhikary, S. K., Rudzionis, Z., & Ghosh, R. (2021). Influence of CNT, graphene nanoplate and CNT-graphene nanoplate hybrid on the properties of lightweight concrete. *Materials Today: Proceedings, 44*, 1979–1982.

Asim, M., Uddin, G. M., Jamshaid, H., Raza, A., Rehman Tahir, Z. U., Hussain, U., Satti, A. N., Hayat, N., & Arafat, S. M. (2020). Comparative experimental investigation of natural fibers reinforced light weight concrete as thermally efficient building materials. *Journal of Building Engineering, 31*, 101411.

Askari Dolatabad, Y., Kamgar, R., & Gouhari Nezad, I. (2020). Rheological and mechanical properties, acid resistance and water penetrability of lightweight self-compacting concrete containing nano-SiO 2, nano-Tio 2 And nano-Al2O3. *Iranian Journal of Science and Technology, Transactions of Civil Engineering, 44*, 603–618.

ASTM C. (1998). *1018 standard test method for flexural toughness and first-crack strength of fiber reinforced concrete.* American Society of Testing and Materials.

ASTM-C330-00. (2017). *Standard specification for lightweight aggregates for structural concrete.* ASTM International.

Chu, H., Qin, J., Gao, L., Jiang, J., Wang, F., & Wang, D. (2023). Effects of graphene oxide on mechanical properties and microstructure of ultra-high-performance lightweight concrete. *Journal of Sustainable Cement-Based Materials, 12*(6), 647–660.

Cui, W., Zhao, L., & Ge, Y. (2023a). Wind-induced buffeting vibration of long-span bridge considering geometric and aerodynamic nonlinearity based on reduced-order modeling. *Journal of Structural Engineering, 149*(11), 04023160.

Cui, W., Zhao, L., Ge, Y., & Xu, K. (2023b). A generalized van der Pol nonlinear model of vortex-induced vibrations of bridge decks with multistability. *Nonlinear Dynamics, 14*, 1–14.

Di Maida, P., Sciancalepore, C., Radi, E., & Bondioli, F. (2018). Effects of nano-silica treatment on the flexural post cracking behaviour of polypropylene macro-synthetic fibre reinforced concrete. *Mechanics Research Communications, 88*, 12–18.

Du, H., Du, S., & Liu, X. (2015). Effect of nano-silica on the mechanical and transport properties of lightweight concrete. *Construction and Building Materials, 82*, 114–122.

Du, X., & Jin, L. (2021). Methodology: meso-scale simulation approach. *Size effect in concrete materials and structures* (pp. 27–76). Springer

Ebrahimkhani, M., Ghiri, A. A., & Farahmand, F. (2020). Finite element analysis of a hip joint prosthesis with an extramedullary fixation system. In *2020 27th National and 5th International Iranian Conference on Biomedical Engineering IICBME*), IEEE.

Esmaeili, J., & Andalibi, K. (2013). Investigation of the effects of nano-silica on the properties of concrete in comparison with micro-silica. *International Journal of Nano Dimension, 3*(4), 321–328.

Esmaeili, J., & Andalibi, K. (2019). Development of 3D Meso-Scale finite element model to study the mechanical behavior of steel microfiber-reinforced polymer concrete. *Computers and Concrete, An International Journal, 24*(5), 413-422.

Esmaeili, J., Sharifi, I., Andalibi, K., & Kasaei, J. (2017). Effect of different matrix compositions and micro steel fibers on tensile behavior of textile reinforced concrete. *IOP Conference Series: Materials Science and Engineering, 246*(1), 012031. IOP Publishing.

Esmaeili, J., Andalibi, K., Gencel, O., Maleki, F. K., & Maleki, V. A. (2021). Pull-out and bond-slip performance of steel fibers with various ends shapes embedded in polymer-modified concrete. *Construction and Building Materials, 271*, 121531.

Hamada, H., Alattar, A., Yahaya, F., Muthusamy, K., & Tayeh, B. A. (2021). Mechanical properties of semi-lightweight concrete containing nano-palm oil clinker powder. *Physics and Chemistry of the Earth, Parts a/b/c, 121*, 102977.

Haydar, A. (2021). Meso-scale finite element modelling of carbon nanotube reinforced polymer composites, Middle East Technical University.

He, H., Shi, J., Yu, S., Yang, J., Xu, K., He, C., & Li, X. (2024). Exploring green and efficient zero-dimensional carbon-based inhibitors for carbon steel: From performance to mechanism. *Construction and Building Materials, 411*, 134334.

He, H., Shuang, E., Wen, T., Yao, J., Wang, X., He, C., & Yu, Y. (2023). Employing novel N-doped graphene quantum dots to improve chloride binding of cement. *Construction and Building Materials, 401*, 132944.

Huang, H., Guo, M., Zhang, W., & Huang, M. (2022). Seismic behavior of strengthened RC columns under combined loadings. *Journal of Bridge Engineering, 27*(6), 05022005.

Ramazani *et al. Int J Concr Struct Mater*   (2024) 18:37

Page 15 of 16

Huang, H., Yuan, Y., Zhang, W., & Li, M. (2021). Seismic behavior of a replaceable artificial controllable plastic hinge for precast concrete beam-column joint. *Engineering Structures, 245*, 112848.

Kalpana, M., & Tayu, A. (2020). Light weight steel fibre reinforced concrete: A review. *Materials Today: Proceedings, 22*, 884–886.

Khani, N., Yildiz, M., & Koc, B. (2016). Elastic properties of coiled carbon nanotube reinforced nanocomposite: A finite element study. *Materials & Design, 109*, 123–132.

Khorshidi, M., Ameri, M., & Goli, A. (2023a). Cracking performance evaluation and modelling of RAP mixtures containing different recycled materials using deep neural network model. *Road Materials and Pavement Design, 15*, 1–20.

Khorshidi, M., Goli, A., Orešković, M., Khayambashi, K., & Ameri, M. (2023b). Performance evaluation of asphalt mixtures containing different proportions of alternative materials. *Sustainability, 15*(18), 13314.

Laipan, M., Yu, J., Zhu, R., Zhu, J., Smith, A. T., He, H., O'Hare, D., & Sun, L. (2020). Functionalized layered double hydroxides for innovative applications. *Materials Horizons, 7*(3), 715–745.

Li, D., Nie, J.-H., Wang, H., & Ren, W.-X. (2024). Loading condition monitoring of high-strength bolt connections based on physics-guided deep learning of acoustic emission data. *Mechanical Systems and Signal Processing, 206*, 110908.

Liao, Y., Yao, J., Deng, F., Li, H., Wang, K., & Tang, S. (2023). Hydration behavior and strength development of supersulfated cement prepared by calcined phosphogypsum and slaked lime. *Journal of Building Engineering, 80*, 108075.

Lin, J.-X., Chen, G., Pan, H.-S., Wang, Y.-C., Guo, Y.-C., & Jiang, Z.-X. (2023). Analysis of stress-strain behavior in engineered geopolymer composites reinforced with hybrid PE-PP fibers: A focus on cracking characteristics. *Composite Structures, 323*, 117437.

Luo, Y., Liu, X., Chen, F., Zhang, H., & Xiao, X. (2023). Numerical simulation on crack-inclusion interaction for rib-to-deck welded joints in orthotropic steel deck. *Metals, 13*(8), 1402.

Maleki, F. K., Nasution, M. K., Gok, M. S., & Maleki, V. A. (2022). An experimental investigation on mechanical properties of Fe2O3 microparticles reinforced polypropylene. *Journal of Materials Research and Technology, 16*, 229–237.

Mohamed, A. M., Tayeh, B. A., Aisheh, Y. I. A., & Salih, M. N. A. (2023). Exploring the performance of steel fiber reinforced lightweight concrete: A case study review. *Case Studies in Construction Materials, 18*, e01968.

Naderi, S., Tu, W., & Zhang, M. (2021). Meso-scale modelling of compressive fracture in concrete with irregularly shaped aggregates. *Cement and Concrete Research, 140*, 106–117.

Othuman Mydin, M. A., Mohd Nawi, M. N., Mohamed, O., & Sari, M. W. (2022). Mechanical properties of lightweight foamed concrete modified with magnetite (Fe3O4) nanoparticles. *Materials, 15*(17), 5911.

Pang, B., Zheng, H., Jin, Z., Hou, D., Zhang, Y., Song, X., Sun, Y., Liu, Z., She, W., & Yang, L. (2024). Inner superhydrophobic materials based on waste fly ash: Microstructural morphology of microetching effects. *Composites Part B: Engineering, 268*, 111089.

Peng, Y., Tang, S., Huang, J., Tang, C., Wang, L., & Liu, Y. (2022). Fractal analysis on pore structure and modeling of hydration of magnesium phosphate cement paste. *Fractal and Fractional, 6*(6), 337.

Pourreza, T., Alijani, A., Maleki, V. A., & Kazemi, A. (2021). Nonlinear vibration of nanosheets subjected to electromagnetic fields and electrical current. *Advances in Nano Research, 10*(5), 481–491.

Prestera, J. R., Boyle, M., Crocker, D. A., Chairman, S. B., Abdun-Nur, E. A., Barton, S. G., Bell, L. W., Blas Jr, S. J., Berg, G. R. & Carrasquillo, P. M. (1998). Standard practice for selecting proportions for structural lightweight concrete (ACI 211.2-98).

Quercia, G., Hüsken, G., & Brouwers, H. (2012). Water demand of amorphous nano silica and its impact on the workability of cement paste. *Cement and Concrete Research, 42*(2), 344–357.

Razi, S., Wang, X., Mehreganian, N., Tootkaboni, M., & Louhghalam, A. (2023). Application of mean-force potential lattice element method to modeling complex structures. *International Journal of Mechanical Sciences, 260*, 108653.

Ren, C., Yu, J., Liu, X., Zhang, Z., & Cai, Y. (2022). Cyclic constitutive equations of rock with coupled damage induced by compaction and cracking. *International Journal of Mining Science and Technology, 32*(5), 1153–1165.

Saghafian, M., Seyedzadeh, H., & Moradmand, A. (2023). Numerical simulation of electroosmotic flow in a rectangular microchannel with use of magnetic and electric fields. *Scientia Iranica*. https://doi.org/10.24200/sci.2023.58474.5742

Shahpari, M., Bamonte, P., & Mosallam, S. J. (2022). An experimental study on mechanical and thermal properties of structural lightweight concrete using carbon nanotubes (CNTs) and LECA aggregates after exposure to elevated temperature. *Construction and Building Materials, 346*, 128376.

Sldozian, R. J. A., Hamad, A. J., & Al-Rawe, H. S. (2023). Mechanical properties of lightweight green concrete including nano calcium carbonate. *Journal of Building Pathology and Rehabilitation, 8*(1), 3.

Tang, S., Yao, Y., Chen, T., Kong, D., Shen, W., & Lee, H. K. (2020). Recent advances in the application of layered double hydroxides in analytical chemistry: A review. *Analytica Chimica Acta, 1103*, 32–48.

Tang, Y., Wang, Y., Wu, D., Chen, M., Pang, L., Sun, J., Feng, W., & Wang, X. (2023). Exploring temperature-resilient recycled aggregate concrete with waste rubber: An experimental and multi-objective optimization analysis. *Reviews on Advanced Materials Science, 62*(1), 20230347.

Vahidi Pashaki, P., Pouya, M., & Maleki, V. A. (2018). High-speed cryogenic machining of the carbon nanotube reinforced nanocomposites: Finite element analysis and simulation. *Proceedings of the Institution of Mechanical Engineers, Part c: Journal of Mechanical Engineering Science, 232*(11), 1927–1936.

Wang, L., Guo, F., Yang, H., Wang, Y., & Tang, S. (2021). Comparison of fly ash, PVA fiber, MgO and shrinkage-reducing admixture on the frost resistance of face slab concrete via pore structural and fractal analysis. *Fractals, 29*(02), 2140002.

Wang, M., Yang, X., & Wang, W. (2022). Establishing a 3D aggregates database from X-ray CT scans of bulk concrete. *Construction and Building Materials, 315*, 125740.

Wu, Z., Huang, B., Fan, J., & Chen, H. (2023). Homotopy based stochastic finite element model updating with correlated static measurement data. *Measurement, 210*, 112512.

Wu, Z., Zhang, J., Fang, Q., Yu, H., & Ma, H. (2021). 3D mesoscopic modelling on the dynamic properties of coral aggregate concrete under direct tension. *Engineering Fracture Mechanics, 247*, 107–136.

Xiao, C., Zheng, K., Chen, S., Li, N., Shang, X., Wang, F., Liang, J., Khan, S. B., Shen, Y., & Lu, B. (2023). Additive manufacturing of high solid content lunar regolith simulant paste based on vat photopolymerization and the effect of water addition on paste retention properties. *Additive Manufacturing, 71*, 103607.

Yang, L., Ye, M., Huang, Y., & Dong, J. (2023). Study on mechanical properties of displacement-amplified mild steel bar joint damper. *Iranian Journal of Science and Technology, Transactions of Civil Engineering, 22*, 1–14.

Yao, Y., Zhou, L., Huang, H., Chen, Z., & Ye, Y. (2023). *Cyclic performance of novel composite beam-to-column connections with reduced beam section fuse elements*. Elsevier.

Zhang, H., Xiang, X., Huang, B., Wu, Z., & Chen, H. (2023a). Static homotopy response analysis of structure with random variables of arbitrary distributions by minimizing stochastic residual error. *Computers & Structures, 288*, 107153.

Zhang, X., Liu, X., Zhang, S., Wang, J., Fu, L., Yang, J., & Huang, Y. (2023b). Analysis on displacement-based seismic design method of recycled aggregate concrete-filled square steel tube frame structures. *Structural Concrete*. https://doi.org/10.1002/suco.202200720

Zhang, X., Zhou, G., Liu, X., Fan, Y., Meng, E., Yang, J., & Huang, Y. (2023c). Experimental and numerical analysis of seismic behaviour for recycled aggregate concrete filled circular steel tube frames. *Computers and Concrete, 31*(6), 537–543.

Zhao, C., Wang, Z., Zhu, Z., Guo, Q., Wu, X., & Zhao, R. (2023). Research on different types of fiber reinforced concrete in recent years: An overview. *Construction and Building Materials, 365*, 130075.

Zhou, C., Wang, J., Shao, X., Li, L., Sun, J., & Wang, X. (2023a). The feasibility of using ultra-high performance concrete (UHPC) to strengthen RC beams in torsion. *Journal of Materials Research and Technology, 24*, 9961–9983.

Zhou, Y., Li, W., Peng, Y., Tang, S., Wang, L., Shi, Y., Li, Y., Wang, Y., Geng, Z., & Wu, K. (2023b). Hydration and fractal analysis on low-heat portland cement pastes using thermodynamics-based methods. *Fractal and Fractional, 7*(8), 606.

Pari Ramazani   Ph. D student at the Department of Civil Engineering, Tabriz Branch, Islamic Azad University, Tabriz, Iran

Moradi Shaghaghi   Assistant Professor at the Department of Civil Engineering, Tabriz Branch, Islamic Azad University, Tabriz, Iran

Masood Farzam   Assistant Professor at the Faculty of Civil Engineering, University of Tabriz, Tabriz, Iran

Hassan Afshin   Assistant Professor at the Faculty of Civil Engineering, Sahand University of Technology, Tabriz, Iran

Mohammad A. Behnajady   Assistant Professor at the Department of Chemistry, Tabriz Branch, Islamic Azad University, Tabriz, Iran